

Fast particle Bremsstrahlung effects in the PIC code EPOCH: Enhanced diagnostics for laser-solid interaction modelling.

Contact N.J.Sircombe@awe.co.uk

R Ward

AWE, Aldermaston, Reading, Berkshire, RG7 4PR, UK.

N J Sircombe

AWE, Aldermaston, Reading, Berkshire, RG7 4PR, UK.

Centre for Fusion, Space & Astrophysics, University of
Warwick, Coventry, CV4 7AL, UK.

Introduction

Particle in Cell (PIC) codes such as EPOCH [1] are key tools for understanding laser plasma interaction in both long and short pulse driven high energy density physics (HEDP) experiments on laser systems such as Orion, Vulcan, NIF and Omega.

Comparison of modelling with experiment is challenging – key processes captured in the code cannot be directly observed experimentally. This is particularly acute in the case of Short Pulse (SP) experiments [2], due to the spatial and temporal scales involved. Diagnosing SP experiments often relies on observations of secondary processes absent from a standard PIC model.

The framework developed within EPOCH to model QED effects at ultra-high intensities [3], provides a robust and computationally tractable mechanism for the generation and tracking of photon macro-particles from atomic and nuclear processes.

Here we demonstrate the feasibility of utilising this framework to generate in-line diagnostics, focussing initially on bremsstrahlung emission from hot electrons.

The Model

EPOCH's QED physics package has been shown to accurately reproduce processes such as quantum corrected synchrotron radiation and multi-photon Breit-Wheeler pair production [3].

The transport of photon macro-particles is easily handled by a fixed-velocity PIC particle push. The generation of photons is handled via a Monte-Carlo approach.

Photon emission is described by Poisson statistics, the cumulative probability of emission over the time taken to traverse an optical depth, τ_{em} , is given by:

$$P(t) = 1 - e^{-\tau_{em}}$$

The initial optical depth term is fixed by assigning P a pseudorandom value from 0 to 1 and inverting, the optical depth for particles can then be updated via a first order integration of:

$$\tau(t) = \int_0^t \lambda(t') dt',$$

where λ is the reaction rate. When the optical depth reaches zero a photon is emitted with an energy sampled from a tabulated spectrum. The new photon is generated co-incident with the generating particle and with equal weight. The generating particle's energy is adjusted accordingly.

Reaction rate and energy spectrum

The reaction rate is determined by the integrated radiation cross section σ_{rad} and the energy spectrum is determined by random sampling of normalised spectra, tabulated in Z , T (particle energy) and k (photon energy) derived from differential cross sections. The integrated and differential cross sections are interpolated from the tables published by Seltzer and Berger[4], based on a review of work carried out by Koch and Motz [5].

Bremsstrahlung emission from Tantalum targets

The approach described above was used to model bremsstrahlung emission from short-pulse irradiated tantalum foils. We consider incident energies of both 25 and 50J, and keep fixed the pulse length (0.7ps), pulse shape (top-hat with a 0.05ps rise), spot-size (8 μ m FWHM) and wavelength (1.054 μ m); adjusting only the intensity.

The targets were 100 μ m thick and angled at 35° to laser normal. They were initialised with a 5 μ m exponential density profile at the front, rising to solid density for the bulk of the target. The target has a fixed ionisation of $Z^*=1$; while EPOCH does have both ionisation [6] and collisional physics modules, neither were employed here in order to focus on the new bremsstrahlung model. The simulation domain measured 256 μ m by 150 μ m with 6400 cells in x and 3200 cells in y , the system boundaries were chosen to be thermal for charged macro-particles, open for photon macro-particles and outflow for fields.

A particle migration algorithm is used to partition the electrons into 'hot' and 'background' populations. While both populations are subject to the same PIC particle push, and can all interact with the laser field, only electrons in the 'hot' population are considered by the bremsstrahlung module. Electrons are promoted from the background to the hot population when they achieve a velocity with magnitude greater than $5v_{Te}$, where v_{Te} is the thermal velocity of the background population in the cell. Electrons can also be demoted from the hot population to the background should their velocity fall below $4v_{Te}$. Not only does this approach have advantages for modelling short pulse LPI, facilitating the characterisation of the hot electron population and greatly simplifying the process of linking PIC and transport codes (as explained in [6]) but it also ensures that the bremsstrahlung model does not consume compute resources dealing with low energy particles of little interest in this context. At lower energies, thermal bremsstrahlung losses can more easily be included in PIC codes, see for example [8], in a macroscopic fashion.

Figure 1 shows the evolution of the target in both the 25J and 50J case, including the hot electron, background electron and photon densities. Hot electrons are generated from the background population as the laser is absorbed in the density

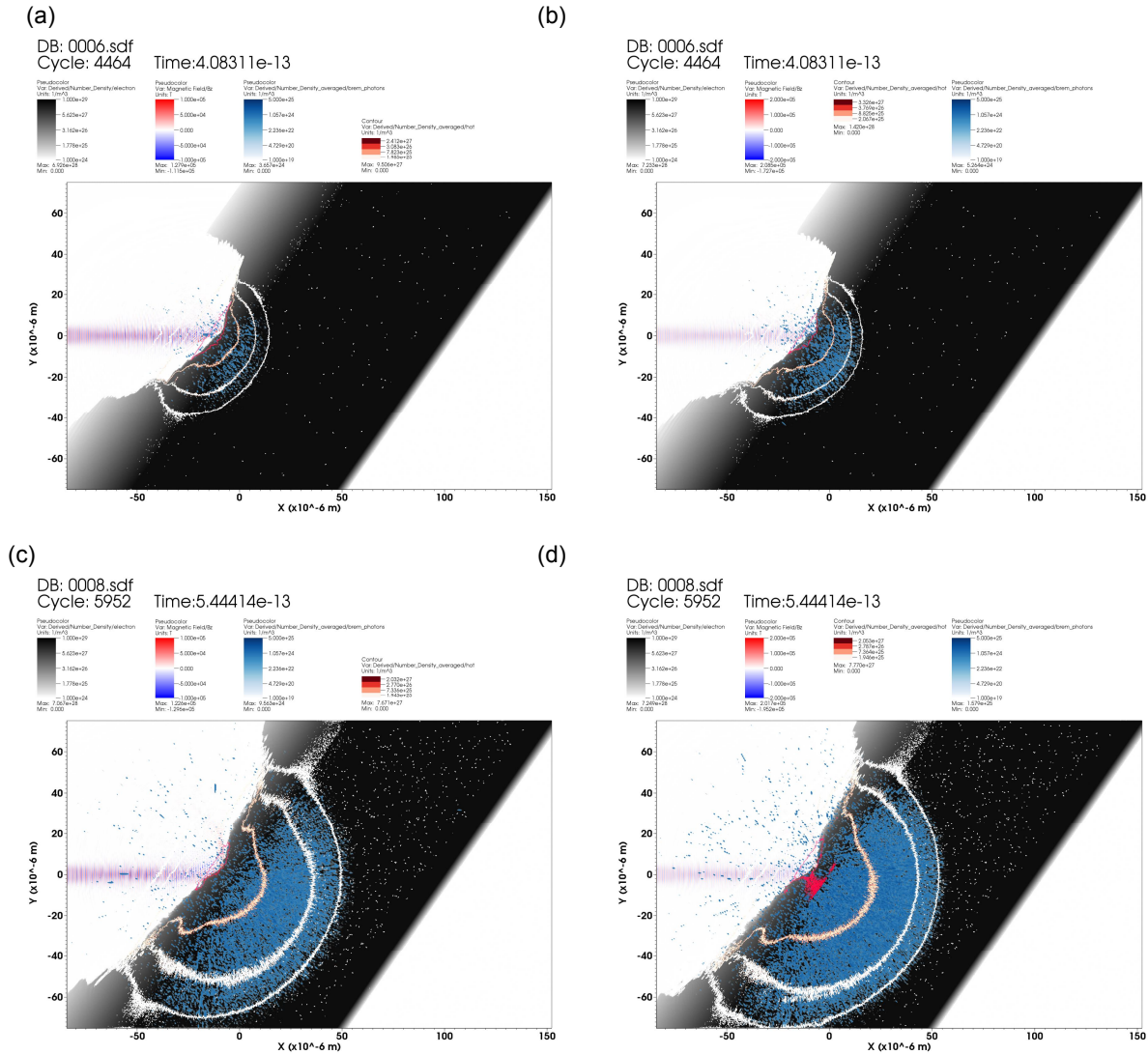


Figure 1: EPOCH simulations of SP-LPI including bremsstrahlung emission, for the case of 25J (‘a’ and ‘c’) and 50J (‘b’ and ‘d’) irradiation. Shown is the laser’s transverse magnetic field, the background electron density, the bremsstrahlung photon density and the hot electron density.

ramp at the front of the target. This population is highly divergent and spreads into the bulk of the target. As the hot electrons interact with the Ta ion population which constitutes the bulk of the target, photon macro-particles are generated as described above. These are pushed through the mesh and recorded when they reach the system boundaries, before being destroyed. In this case, by choice, the photons do not interact with each other, the charged macro-particles or the classical fields stored on the computational mesh, however the QED model in EPOCH is capable of modelling a number of processes, as described in [3], and these models could be used in conjunction with the fast particle bremsstrahlung model in future.

A hot electron probe diagnostic, placed behind the laser absorption region, records the properties of the hot electrons generated by the laser as they pass into the bulk target. Figure 2 Shows the energy spectrum for both the 25J and 50J cases, as well as an example with no bremsstrahlung module in use.

The hotter tail present in the 50J case is as a result of the higher laser intensity. This is reflected in the photon energy spectrum (see Figure 3). The characteristic energy of the exponential fits to the tails of the electron and photon spectra in each case indicates that the gamma-ray emission from such targets may serve as a diagnostic on the high energy electrons generated at the target surface, free from the effects of any rear-surface

interactions which may influence results from electron spectrometers.

The conversion efficiencies observed are summarised in Table 1. The two cases are roughly equivalent, with only a small fraction (~0.2%) of the incident laser energy being converted into bremsstrahlung photons. In both cases, the bulk of this energy is in the gamma-ray range (see Table 2). In the 50J case, the conversion efficiency into both soft and hard X-rays is lower, with a larger fraction of the incident energy being converted into gamma rays. This is due to high energy tail observed in the electron distribution. These multiple-MeV electrons are able to transit and leave the target while retaining much of their energy. Thicker targets would be able to convert a higher fraction of this hot electron energy. However, in practice, the additional target thickness would increase the absorption of lower energy photons. Thinner targets, on the other hand, would reduce the re-absorption of soft X-rays and suppress the generation of gamma rays generating a softer spectrum overall. A ‘cooling’ of the hot electron spectrum may also be desirable in some cases to try and increase the conversion efficiency into X-Rays. This could be achieved by a conversion to a shorter wavelength or by a reduction in the level of pre-plasma present when the main pulse arrives – although the pre-plasma in these simulations was prescribed, in practice the extent of any pre-plasma can be minimised by the adoption of a higher contrast pulse.

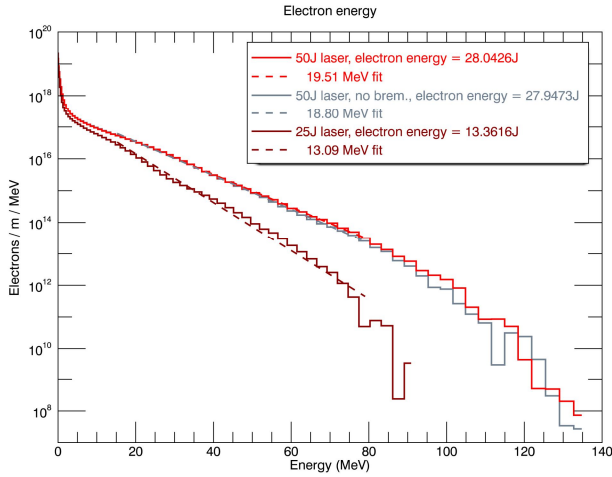


Figure 2: Time integrated electron energy spectra recorded behind the absorption region for both the 25J and 50J cases. The 50J case has been repeated with the bremsstrahlung package disabled. The small reduction in absorbed energy in this case is most likely due to the stochastic nature of the simulation.

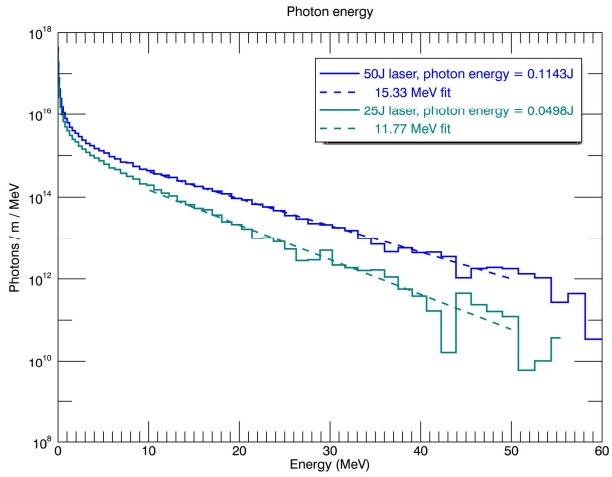


Figure 3: Time integrated Photon spectra in each case, generated using all photons which leave the system anywhere to the behind the target’s front surface. A small number of photons are observed which propagate back towards the laser, these are generated from refluxing electrons, have a softer spectrum and account for less than 0.02% of the incident laser energy.

Laser	Energy (J)		Conversion efficiency		
	Hot electrons	Photons	Laser to hot electrons	Hot electrons to brems. photons	Laser to brems. photons
25	13.36	0.05	53.45%	0.37%	0.20%
50	28.04	0.11	56.09%	0.41%	0.23%

Table 1: No significant difference in the conversion efficiencies for incident laser to hot electrons, hot electrons to bremsstrahlung photons and laser to bremsstrahlung photons was observed.

Laser	Energy (J)		
	Soft X-ray	Hard X-ray	Gamma
25	5.14E-06 (0.000021%)	1.98E-04 (0.00079%)	4.96E-02 (0.1984%)
50	6.77E-06 (0.000014%)	2.88E-04 (0.00058%)	1.14E-01 (0.2280%)

Table 2: Conversion efficiency into soft X-ray (1-5keV), hard X-ray (5-50keV) and gamma ray (>50keV) photons.

Conclusions

The simulations presented here highlight the potential of EPOCH’s QED physics framework to provide inline diagnostics for direct comparison with experiments.

While we have focussed on bremsstrahlung emission from high energy electrons, the approach could readily be extended to processes such as $K\alpha$ emission and coherent transition radiation. Future work could also include the development of post processing capability to include point-of-view effects and convolve in detector response.

There is a computational overhead in including photon tracking, but in the cases discussed here, this amounted to less than a 10% slow-down – aided by the inclusion of open photon boundaries, distinct from the charged particle boundary conditions.

Results from simulations of bremsstrahlung emission from the short-pulse irradiation of Ta foils shows that the conversion efficiency in thin targets is low, and dominated by conversion to gamma rays under the conditions adopted. While higher conversion efficiencies would be expected for thicker targets, this would be accompanied by increased absorption of lower energy photons. A softer spectrum could be achieved via modifications to the laser parameters (such as lowering intensity, conversion to higher harmonics and higher contrast beams, in order to minimise pre-plasma generation), or the use of a thinner target.

The high energy tail of the photon distribution observed in simulations also reflects the characteristics of the electron distribution at the laser-plasma interaction region and provides a potential diagnostic on the hot electron source, and a point of comparison between simulation and experiment.

Acknowledgements

The authors would like to thank C S Brady, D Neely, L Wilson, D Rusby and C Brenner for their helpful discussions during the course of conducting this work.

© British Crown Owned Copyright 2014/AWE.

References

1. www.ccpp.ac.uk
2. C. D. Chen *et al.* “Comparisons of angularly and spectrally resolved Bremsstrahlung measurements to two-dimensional multi-stage simulations of short-pulse laser-plasma interactions”, *Phys. Plasmas*, 20, 052703 (2013)
3. C. P. Ridgers *et al.* “Modelling gamma-ray photon emission and pair production in high-intensity laser-matter interactions”, *J. Comput. Phys.*, 260, 273 (2014)
4. S. M. Seltzer and M.J. Berger. “Bremsstrahlung spectra from electron interactions with screened atomic nuclei”, *Nuclear Instruments and Methods in Physics Research*, B12, 95 (1985).
5. Koch and Motz, “Bremsstrahlung cross-section formulas and related data”, *Review of Modern Physics*, 31, 4 (1959)
6. N. J. Sircombe, S. J. Hughes and M. G. Ramsay, “Integrated calculations of short-pulse laser” interactions with matter”, *New Journal of Physics*, 15, 025025 (2013)
7. C. S. Brady, A. Lawrence-Douglas, and T. D. Arber, “Rapid filamentation of high power lasers at the quarter critical surface”, *Phys. Plasmas*, 19, 063112 (2012)
8. R. Mishra *et al.* “Collisional particle-in-cell modeling for energy transport accompanied by atomic processes in dense plasmas.” *Phys. Plasmas*, 20, 072704, (2013).